

# Design of Constant Beamwidth Beamformers in Elevation Angle with Concentric Ring Arrays

Orel Peretz



# Design of Constant Beamwidth Beamformers in Elevation Angle with Concentric Ring Arrays

Research Thesis

Submitted in partial fulfillment of the requirements  
for the degree of Master of Science in Electrical Engineering

**Orel Peretz**

Submitted to the Senate  
of the Technion — Israel Institute of Technology  
Iyar 5785      Haifa      May 2025



This research was carried out under the supervision of Prof. Israel Cohen, in the Faculty of Electrical and Computer Engineering.

Some results in this thesis have been published as an article by the author and research collaborator in a journal during the course of the author's masters research period, the most up-to-date version of which being:

O. Peretz and I. Cohen, "Constant elevation-beamwidth beamforming with concentric ring arrays," <i>IEEE/ACM Transactions on Audio, Speech, and Language Processing</i> , vol. 32, pp. 1662–1672, 2024.
--

The author of this thesis states that the research, including the collection, processing and presentation of data, addressing and comparing to previous research, etc., was done entirely in an honest way, as expected from scientific research that is conducted according to the ethical standards of the academic world. Also, reporting the research and its results in this thesis was done in an honest and complete manner, according to the same standards.

## Acknowledgements

This thesis was done under the supervision of Prof. Israel Cohen in the Department of Electrical and Computer Engineering.

I would like to express my deepest gratitude and appreciation to my research supervisor, Prof. Israel Cohen for the opportunity, his supervision, support, and patience throughout the stages of this research. His expertise, guidance, and support have made me a significantly better researcher.

Lastly, I would like to thank my family for supporting and encouraging me through this process. This accomplishment would not have been possible without them.

The generous financial support of the Technion, the ISF-NSFC joint research program (grant No. 1449/23), and the Pazy Research Foundation is gratefully acknowledged.



# Contents

## List of Figures

<b>Abstract</b>	<b>1</b>
<b>Abbreviations</b>	<b>3</b>
<b>Notations</b>	<b>5</b>
<b>1 Introduction</b>	<b>7</b>
1.1 Background and Motivation . . . . .	7
1.2 Main Contributions . . . . .	8
1.3 Research Overview . . . . .	9
1.4 Organization . . . . .	10
<b>2 Preliminaries</b>	<b>11</b>
2.1 Concentric Ring Array . . . . .	11
2.2 Signal Model . . . . .	12
2.3 Performance Measures . . . . .	14
2.4 Genetic Algorithms . . . . .	15
<b>3 Constant Elevation-Beamwidth Beamforming with CRAs</b>	<b>17</b>
3.1 Constant-Beamwidth Beampattern Design . . . . .	17
3.1.1 Time Domain Filter Design . . . . .	17
3.1.2 Optimization Constraints . . . . .	19
3.1.3 Objective Function . . . . .	20
3.2 Hybrid Optimization using Genetic Algorithm . . . . .	20
3.3 Experimental Results . . . . .	23
3.3.1 Influence of $\alpha$ . . . . .	23
3.3.2 Influence of $L$ . . . . .	26
3.3.3 Sidelobe Level Comparison . . . . .	26
3.3.4 Hybrid Approach . . . . .	26

<b>4</b>	<b>Conclusions</b>	<b>33</b>
4.1	Summary . . . . .	33
4.2	Future Research . . . . .	34
	<b>Hebrew Abstract</b>	<b>i</b>

# List of Figures

2.1	Illustration of a CRA with $M$ rings and $N_m$ microphones per ring. . . .	12
2.2	Block diagram of CRA FIR-beamformer. . . . .	13
3.1	(a-c) Beampatterns of the proposed beamformer for a non-uniform CRA with $M = 5$ rings and $L = 32$ filter taps. The overlaid dashed line is the half-power contour of the mainlobe. (d-f) Weight values are applied to the rings at each frequency. . . . .	24
3.2	Performance measures of the proposed beamformer with $\alpha = 1$ (square), $\alpha = 0.3$ (diamond), $\alpha = 0.15$ (cross), $\alpha = 0$ (asterisk), and Kleiman [40] (circle) for $L = 32$ filter taps. (a) DF, (b) WNG, and (c) Beamwidth $\theta_{BW}$ , as a function of frequency. . . . .	25
3.3	Performance measures of the proposed beamformer with $\alpha = 1$ (square), $\alpha = 0.3$ (diamond), $\alpha = 0.15$ (cross), $\alpha = 0$ (asterisk), and Kleiman [40] (circle) for $L = 20$ filter taps. (a) DF, (b) WNG, and (c) Beamwidth $\theta_{BW}$ , as a function of frequency. . . . .	27
3.4	Beampatterns at different frequencies in range $[1.4, 7.6]$ kHz with $L = 32, \alpha = 1$ . The solid line marks the sidelobe level. . . . .	28
3.5	Performance measures of the proposed hybrid approach with $\alpha = 1$ (square), $\alpha = 0.3$ (diamond), $\alpha = 0.15$ (cross) and $\alpha = 0$ (asterisk) for $L = 32$ filter taps. (a) DF, (b) WNG, and (c) Beamwidth $\theta_{BW}$ , as a function of frequency. . . . .	29
3.6	Convergence plot. Cost value versus the number of generations obtained by the proposed hybrid approach. The solid line and the shaded area are the mean and standard deviation of the cost over 100 MC runs, respectively. . . . .	30



# Abstract

Beamforming is a classical method for spatial filtering of a desired signal from noise and interference using observations from multiple microphones. By applying appropriate delays and weights to the microphone signals, the array can be steered spatially to focus on the desired sound source. This directional filtering improves signal quality and intelligibility, making beamforming essential in many audio and communication systems. It has been widely adopted in applications such as hands-free telephony, hearing aids, and smart conferencing devices. Real-world scenarios often involve broadband signals in 3D environments, requiring efficient solutions for low latency, minimum resources, and high performance.

Conventional beamforming suffers from beamwidth narrowing as frequency increases, which leads to undesired distortion and a low-pass effect for broadband signals arriving from directions other than the intended look direction. To address this issue, several methods have been proposed in the literature for designing beamformers with frequency-invariant or constant beamwidth characteristics. However, some of these methods involve high computational complexity, making them impractical for real-time applications, especially when using large microphone arrays or operating under strict hardware constraints. Other approaches assume that the desired signal's direction of arrival (DOA) lies in the horizontal plane, limiting their effectiveness in full 3D environments and degrading performance metrics such as directivity factor (DF) and white noise gain (WNG). Additionally, array geometry plays a critical role in overall system performance.

This thesis focuses on the efficient design of constant-elevation beamwidth beamformers on concentric ring arrays (CRAs). We adopt the CRA configuration in which an analog summation of all the signals captured by each microphone in a ring is performed before sampling. While eliminating beam steering ability, this design requires fewer resources and significantly simplifies the overall computational complexity, making it highly suitable for real-time and resource-constrained applications. In addition, the beamformer filters are implemented through temporal finite impulse response (FIR) filters, which are better suited for real-time applications requiring small delays. First, we introduce a convex quadratic programming (CQP) problem for a given CRA configuration. Multiple constraints are suggested for shaping the array response, maintaining constant beamwidth over an extensive range of frequencies, and a distortionless response

in the DOA of the signal. We utilized the continuous-phase representation of FIR filters, enabling the joint and direct optimization of the time domain FIR coefficients. The proposed objective function contains a control variable, allowing a tradeoff between the directivity factor and the white noise gain. Subsequently, a hybrid approach is proposed to optimize the ring radii with a genetic algorithm utilizing the aforementioned convex problem as its cost, exploiting the partial convexity of the problem. The design exploits the degrees of freedom of the array geometry for superior performance. In particular, the ring radii and the beamformer coefficients are optimized simultaneously for all frequencies. Experimental results demonstrate the flexibility and advantages of the proposed approach compared to the state-of-the-art in terms of directivity factor, white noise gain, sidelobe level, and beamwidth consistency, with reduced resources and a significantly lower computation time.

# Abbreviations

3D	: Three-Dimensional
CB	: Constant-Beamwidth
CCA	: Concentric Circular Array
CP	: Convex Programming
CQP	: Convex Quadratic Programming
CRA	: Concentric Ring Array
CS	: Compressed Sensing
DF	: Directivity Factor
DMNUM	: Dynamic Multi-Nonuniform Mutation
DOA	: Direction of Arrival
DOF	: Degrees of Freedom
EIC	: Extended Intermediate Crossover
FI	: Frequency Invariant
FIR	: Finite Impulse Response
GA	: Genetic Algorithm
MC	: Monte Carlo
MFO	: Moth Flame Optimization
MIQP	: Mixed Integer Quadratic Programming
PSLL	: Peak Sidelobe Level
PSO	: Particle Swarm Optimization
RA	: Rectangular Array
RS	: Rank-Scaled
SLL	: Sidelobe Level
SUS	: Stochastic Universal Sampling
WNG	: White Noise Gain



# Notations

$A_{BW}$	:	Beamwidth $-3$ dB amplitude
$\mathcal{B}[\mathbf{h}(f), \theta]$	:	The beampattern
$c$	:	Speed of sound
$\mathcal{D}$	:	The broadband directivity factor
$\mathcal{D}(f)$	:	The narrowband directivity factor
$\mathbf{d}(f, \theta)$	:	The steering vector of the $m$ th ring
$f$	:	Frequency
$f(\cdot)$	:	A Function
$H_m(f)$	:	The gain of the $m$ -th ring
$\mathbf{I}_N$	:	The $N \times N$ identity matrix
$\text{Im}\{\cdot\}$	:	The imaginary part of a complex scalar, vector, or matrix
$J_0$	:	Zero-order Bessel function
$j$	:	The imaginary unit
$K$	:	Number of frequency bins
$L$	:	The filter's order
$M$	:	Number of rings
$N$	:	Number of sensors in the array
$N_{elite}$	:	Number of elite chromosomes
$N_{gen}$	:	Number of genes in a chromosome
$N_m$	:	Number of sensors on the $m$ th ring
$N_{pop}$	:	Number of chromosomes in the population
$p_{mu}$	:	Chromosome mutation probability
$p_{mu}^{gene}$	:	Gene mutation probability
$R_m$	:	Radius of the $m$ th ring
$R_{min}$	:	Largest radius in the CRA
$R_{max}$	:	Lowest radius in the CRA
$\text{Re}\{\cdot\}$	:	The real part of a complex scalar, vector, or matrix
$\mathbf{r}_{m,k}$	:	The location of the $m, k$ -th microphone
$s(t)$	:	An acoustic source signal in time domain
$\mathbf{T}$	:	A partitioning preprocessing matrix
$\mathcal{W}$	:	The broadband white noise gain
$\mathcal{W}(f)$	:	The narrowband white noise gain

$x$	: a scalar
$\mathbf{x}$	: A vector
$\mathbf{X}$	: A matrix
$(\mathbf{X})_{i,j}$	: The $i, j$ -th element of a matrix $\mathbf{X}$
$\alpha$	: Tradeoff parameter between WNG and DF
$\gamma$	: Shape parameter of the mutation function
$\mathbf{\Gamma}(f)$	: The pseudo-coherence matrix
$\Theta_{BW}$	: The angles that cover the mainlobe region
$\theta$	: Elevation angle
$\lambda$	: Wavelength
$\lambda_m^{min}$	: Minimal effective wavelength of the $m$ -th ring
$\tau_{m,k}$	: Delay of the $m, k$ -th microphone
$\psi_{m,k}$	: Angle of the $m, k$ -th microphone
$\Phi_{BW}$	: The frequencies that cover the mainlobe region
$\varphi$	: Azimuth angle
$\otimes$	: The Kronecker product
$\circ$	: The Hadamard product
$(\cdot)^H$	: Conjugate transpose operator
$(\cdot)^T$	: Transpose operator
$(\cdot)^*$	: Conjugate operator
$\lceil \cdot \rceil$	: The ceil of a number
$\angle \{ \cdot \}$	: The phase of the complex-valued variable
$\  \cdot \ _2$	: The Euclidean norm
$\mathbf{1}_N$	: The $N \times 1$ all-ones vector

# Chapter 1

## Introduction

### 1.1 Background and Motivation

Beamforming is a classical method for spatial filtering of a desired signal from noise and interference using observations from multiple microphones [1]–[3]. It has been at the forefront of research activity for many decades, applied in applications such as hands-free audio communication, hearing aids, and teleconferencing systems [4], [5]. Most applications involve signals that are broadband in nature in a three-dimensional (3D) setting, requiring efficient solutions for low latency, minimum resources, and high performance.

Conventional beamforming suffers from beamwidth narrowing as frequency increases, causing an undesired distorted low-passed output for signals deviating from the look direction. Over the last few decades, several frequency-invariant (FI) and constant-beamwidth (CB) methods have been suggested with different array geometries, which can be generally divided into three categories: linear [6]–[10], planar [11]–[24] and volumetric [25], [26]. The planar arrays are favored over the others due to their 2D steering ability and limited resources (area, number of elements, etc.). Among the planar array geometries are: the rectangular arrays (RAs) [11]–[17], [27], the circular arrays (CAs) [18]–[20] and the concentric circular arrays (CCAs) [21]–[24]. The last is preferred in many applications due to 360° azimuth coverage and superior performance in direction of arrival (DoA) [21], [28], peak sidelobe level (PSLL) [29], noise suppression [30], and frequency invariance over a wide range of frequencies [31]. However, most works restrict the desired signal DoA to the horizontal plane, affecting the beamformer’s performance in terms of directivity factor (DF) and white noise gain (WNG). In [32], a CB beamformer for CCAs controlling both the azimuth and elevation beamwidths was suggested. Yet, for large arrays, the computational complexity and required resources may be too high due to the large number of degrees of freedom (DOF). A compromise is the concentric ring array (CRA), where all microphones in a ring share the same weight. While eliminating beam steering ability, the number of DOFs is reduced, as are the computational complexity and required resources. In [33], a window-based CB

beamformer for uniformly spaced CRA was suggested.

Generally, two main design controls are affecting the performance of the CRA beamformer: the ring radii and weights. Previous work on beampattern synthesis of CRAs optimizing both radii and weights includes optimization methods such as particle swarm optimization (PSO) [34], compressed sensing (CS) [35], and moth flame optimization (MFO) [36]. Yet, for the most part, these methods are computationally exhaustive for large arrays. Following, hybrid approaches [37]–[39] decomposing the optimization problem into two parts were suggested. In [37], a combination of a genetic algorithm (GA) and convex programming (CP) was proposed, exploiting the convexity of the problem and the parallelism of the GA for improved efficiency. Yang et al. [39] employed the same combination while optimizing the ring partitions in addition to the radii and weights under linear constraints. Unfortunately, all the aforementioned approaches were designed for the narrowband case without beamwidth control. Moreover, they ignore important performance measures such as the DF and WNG.

Recently, Klieman et al. [40] proposed a maximum DF CB beamformer with time-domain implementation by solving a mixed integer quadratic programming (MIQP) problem of both the weights and radii. However, it suffers from several disadvantages. First, the radii are optimized on a grid, which is computationally exhaustive, especially for a large grid. Second, the algorithm comprises two separate optimization problems: one for finding the weights that maximize the DF and the other for finding the finite impulse response (FIR) coefficients approximating the beamformer weights concerning the least-squares cost. Next, the FIR coefficients are designed independently for each ring. Consequently, the final time-domain solution is suboptimal, which may cause a degradation in performance. Lastly, objective function weighting and a pre-processing step are needed to compensate for the non-smooth filter response of the incoherent solution.

Our motivation arises from many multi-speaker applications involving large spaces with speakers distributed across different pre-defined areas such as auditoriums, classrooms, houses of worship, and conference centers. In such scenarios, our beamformer with the eliminated steering ability can be installed as a circular ceiling array over the different regions of interest. This solution benefits from low cost, latency, and high performance [33].

## 1.2 Main Contributions

The research in this thesis focuses on filling in the knowledge gaps discussed in the previous section. We list our main contributions:

- A new formulation of a convex quadratic programming (CQP) problem for the design of a CB FIR beamformer for a given CRA configuration. We utilize the continuous-phase representation of FIR filters, enabling the joint and direct op-

timization of the time domain FIR coefficients.

- We propose an objective function that includes a control variable, allowing a tradeoff between DF and WNG.
- A hybrid approach is proposed to optimize the ring radii with a genetic algorithm utilizing the aforementioned convex problem as its cost and exploiting the partial convexity of the problem. The design exploits the degrees of freedom of the array geometry for superior performance. In particular, the ring radii and the beamformer coefficients are optimized simultaneously for all frequencies.
- To encourage further research we provide an open-source of our work accessible at <https://github.com/PeretzOrel/CB-EL-CRA>.

In the remainder of this chapter, we describe these issues and indicate the design considerations that motivated our work.

### 1.3 Research Overview

The presented research focuses on the efficient design of constant elevation-beamwidth beamformers with CRA. We adopt the CRA configuration in which an analog summation of all the received signals from a given ring is performed before sampling, requiring fewer resources and simplifying the computational complexity. In addition, the beamformer filters are implemented through temporal finite impulse response (FIR) filters, which is better suited for real-time application requiring small delays. First, we utilize the continuous-phase representation of the FIR filters for defining a convex quadratic programming (CQP) problem, maintaining CB over a wide range of frequencies for a given CRA configuration. We propose an objective function that includes a control variable, allowing a tradeoff between DF and WNG. Following, a hybrid approach is proposed to optimize the ring radii with a genetic algorithm utilizing the aforementioned convex problem as its cost and exploiting the partial convexity of the problem. The design exploits the degrees of freedom of the array geometry for superior performance. In particular, the ring radii and the FIR beamformer coefficients are optimized simultaneously for all frequencies. Simulation results compare the proposed approach against the state-of-the-art, showing several advantages. First, the flexibility of the proposed approach is demonstrated, allowing a compromise between DF and WNG. Second, the improved performance in terms of WNG, beamwidth consistency, and sidelobe level (SLL) due to the direct and joint optimization of the coefficients is shown. Lastly, the significantly lower computational time and faster convergence of the proposed approach are demonstrated through independent Monte Carlo (MC) runs.

## 1.4 Organization

This thesis is organized as follows. In Chapter 2 we present the scientific background related to this work. We present the CRA, the signal model, performance measures, and some background on genetic algorithms. Chapter 3 introduces the first original contribution of this research, where an efficient design of CB FIR beamformer is suggested for CRAs. We introduce a convex quadratic programming problem for a given CRA configuration, directly optimizing the beamformer coefficients while maintaining constant elevation-beamwidth over a wide range of frequencies. Subsequently, a hybrid approach is proposed to optimize the ring radii with a genetic algorithm exploiting the partial convexity of the problem. Experimental results demonstrate the flexibility and advantages of the proposed approach compared to the state-of-the-art. Finally, Chapter 4 summarizes the main findings of this research, concludes the thesis, and presents possible directions for future work.

## Chapter 2

# Preliminaries

This chapter provides some background for reading this thesis and briefly describes relevant methods and metrics used in the research. In Section 2.1, we present the required background on array processing with circular geometry. Section 2.2 presents the signal model. Following, Section 2.3 presents the performance measures used for the beamformers evaluations. Finally, Section 2.4 provides the fundamentals of genetic algorithms.

### 2.1 Concentric Ring Array

Consider a discrete CRA with  $M$  rings. The  $m$ -th ( $m = 1, \dots, M$ ) ring has a radius  $R_m$ , containing  $N_m$  equally spaced omnidirectional microphones, as illustrated in Fig. 2.1. We assume that the center of the CRA coincides with the first ring having  $R_1 = 0$  and  $N_1 = 1$ . The total number of microphones in the array is  $N = \sum_{m=1}^M N_m$ .

The location of the  $k$ -th ( $k = 1, \dots, N_m$ ) microphone on the  $m$ -th ring is given by

$$\mathbf{r}_{m,k} = R_m (\cos \psi_{m,k}, \sin \psi_{m,k}, 0)^T \quad (2.1)$$

$$\psi_{m,k} = \frac{2\pi(k-1)}{N_m} \quad (2.2)$$

where  $\psi_{m,k}$  is the angular position, measured anti-clockwise concerning the  $x$ -axis.

To prevent spatial aliasing, the inner-microphone spacing on each ring should satisfy the Nyquist spatial sampling criterion, i.e., be less than  $\lambda_m^{\min}/2$ , where  $\lambda_m^{\min}$  is the minimal wavelength in which the  $m$ -th ring is effective in the beamforming process. Consequently, the number of microphones of the  $m$ -th ring is given by

$$N_m \geq \left\lceil \frac{4\pi R_m}{\lambda_m^{\min}} \right\rceil. \quad (2.3)$$

Since the microphones are spaced uniformly and satisfy the Nyquist criterion, we get an azimuth-invariant beampattern. Therefore, without loss of generality, we choose

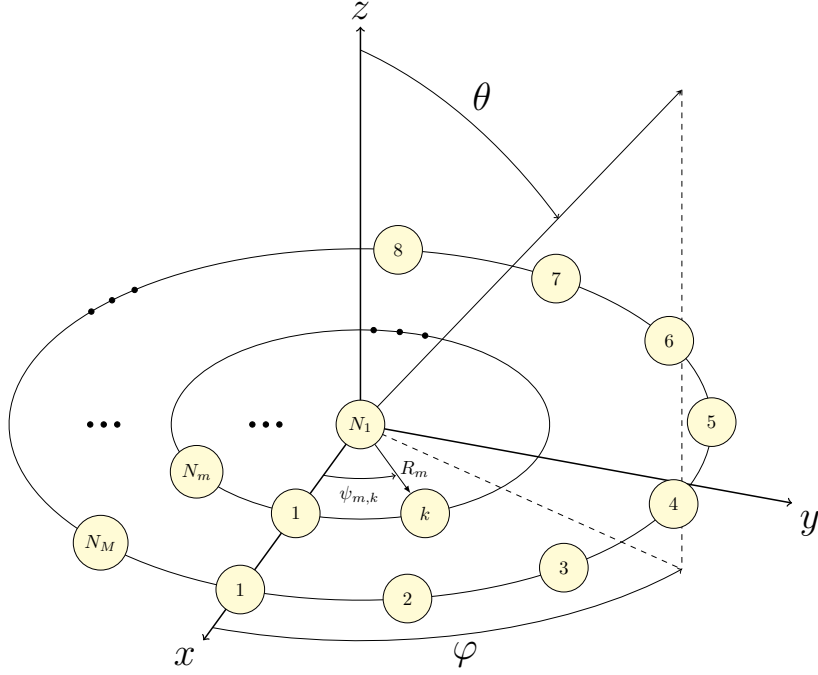


Figure 2.1: Illustration of a CRA with  $M$  rings and  $N_m$  microphones per ring.

$\varphi = 0$  for the rest of this work.

## 2.2 Signal Model

Suppose a desired broadband signal  $s(t)$  propagates in an anechoic acoustic environment at the speed of sound, i.e.,  $c = 340$  m/s, impinges on the CRA. We assume a far-field model so the wave can be approximated as planar. The DoA of the desired signal is parameterized by the elevation angle  $\theta_d$ .

The signal observed by the  $m, k$ -th microphone is a time-delayed version of the original signal corrupted by noise  $v_{m,k}(t)$ , that is

$$x_{m,k}(t) = s(t - \tau_{m,k}) + v_{m,k}(t) \quad (2.4)$$

$$\tau_{m,k} = \frac{R_m}{c} \sin \theta \cos(\psi_{m,k}) \quad (2.5)$$

where  $\tau_{m,k}$  denotes the propagation time difference between the origin and the  $m, k$ -th microphone. Applying the Fourier transform translates the time delay  $\tau_{m,k}$  to a phase shift  $e^{-j2\pi f\tau_{m,k}}$ , that is

$$X_{m,k}(f) = e^{-j2\pi f\tau_{m,k}} S(f) + V_{m,k}(f) \quad (2.6)$$

where  $f$  is the temporal frequency. In vector form, the observed signal of the  $m$ -th ring

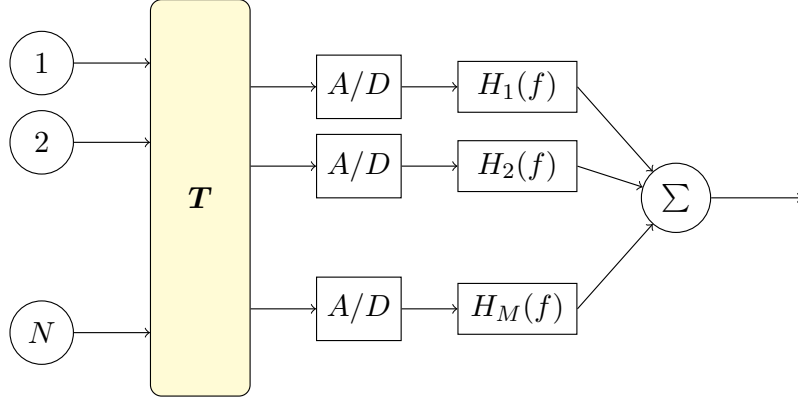


Figure 2.2: Block diagram of CRA FIR-beamformer.

becomes

$$\begin{aligned} \underline{\mathbf{X}}_m(f) &= [X_{m,1}(f), \dots, X_{m,N_m}(f)]^T \\ &= \underline{\mathbf{d}}_m(f, \theta) S(f) + \underline{\mathbf{V}}_m(f) \end{aligned} \quad (2.7)$$

where the vector  $\underline{\mathbf{V}}_m(f)$  is defined similarly to  $\underline{\mathbf{X}}_m(f)$  and  $\underline{\mathbf{d}}_m(f, \theta)$  is the steering vector of the  $m$ -th ring given by

$$\underline{\mathbf{d}}_m(f, \theta) = \begin{bmatrix} e^{j \frac{2\pi f R_m}{c} \sin \theta \cos(\psi_{m,1})} \\ \vdots \\ e^{j \frac{2\pi f R_m}{c} \sin \theta \cos(\psi_{m,N_m})} \end{bmatrix}. \quad (2.8)$$

Concatenating the  $M$  rings steering vectors yields the steering vector of the CRA, which is given by

$$\mathbf{d}(f, \theta) = [\underline{\mathbf{d}}_1^T(f, \theta), \dots, \underline{\mathbf{d}}_M^T(f, \theta)]^T. \quad (2.9)$$

In the proposed beamformer design, the first stage is the summation of all microphone signals of each ring followed by an A/D sampler per ring. Then, in the second stage, each output signal is filtered by an FIR filter. A block diagram of the proposed beamformer design is illustrated in Fig. 2.2. While eliminating beam steering ability, the proposed design requires fewer resources and simplifies the computational complexity. Mathematically, the sum operation can be represented by applying a partitioning preprocessing matrix  $\mathbf{T}$  of size  $N \times M$  to the digital signal, defined as

$$\mathbf{T} = \begin{pmatrix} \mathbf{1}_{N_1}/N_1 & \mathbf{0} & \cdots & \mathbf{0} \\ \mathbf{0} & \mathbf{1}_{N_2}/N_2 & \cdots & \mathbf{0} \\ \vdots & \vdots & \ddots & \vdots \\ \mathbf{0} & \mathbf{0} & \cdots & \mathbf{1}_{N_M}/N_M \end{pmatrix} \quad (2.10)$$

The weight vector at frequency  $f$  of the CRA rings is given by

$$\underline{\mathbf{h}}(f) = [H_1(f), \dots, H_M(f)]^T \quad (2.11)$$

where  $H_m(f)$  is the FIR frequency response at frequency  $f$  applied to the  $m$ -th ring. Using (2.10), the weight vector at frequency  $f$  of the CRA microphones can be expressed as:

$$\mathbf{h}(f) = \mathbf{T}\underline{\mathbf{h}}(f) \quad (2.12)$$

## 2.3 Performance Measures

In this section, we define some relevant performance measures for deriving and analyzing the proposed beamformer.

The beampattern describes the sensitivity of the beamformer to a plane wave impinging on the array from different directions, defined as

$$\begin{aligned} \mathcal{B}[\mathbf{h}(f), \theta] &= \mathbf{h}^H(f) \mathbf{d}(f, \theta) \\ &= \sum_{m=1}^M H_m^*(f) \sum_{k=1}^{N_m} e^{j \frac{2\pi f R_m}{c} \sin \theta \cos(\psi_{m,k})}. \end{aligned} \quad (2.13)$$

When the Nyquist criterion in (2.3) is satisfied, the beampattern can be expressed using the beampattern of continuous rings

$$\mathcal{B}[\mathbf{h}(f), \theta] = \sum_{m=1}^M H_m^*(f) N_m J_0 \left( \frac{2\pi f}{c} R_m \sin \theta \right) \quad (2.14)$$

where  $J_0$  is the zero-order Bessel function.

The (narrowband) WNG quantifies the robustness of the beamformer to imperfections, such as microphone noise, displacement, and mismatch, defined as

$$\mathcal{W}(f) = \frac{|\mathbf{h}^H(f) \mathbf{d}(f, \theta_d)|^2}{\mathbf{h}^H(f) \mathbf{h}(f)}. \quad (2.15)$$

where  $\theta_d$  is the look direction. The broadband WNG is defined as

$$\mathcal{W} = \frac{\int_f |\mathbf{h}^H(f) \mathbf{d}(f, \theta_d)|^2 df}{\int_f \mathbf{h}^H(f) \mathbf{h}(f) df}. \quad (2.16)$$

Another important measure is the (narrowband) DF, which quantifies how the sen-

array performs in the presence of reverberation, defined as

$$\begin{aligned} \mathcal{D}(f) &= \frac{|\mathcal{B}(f, \theta_d, \phi_d)|^2}{\frac{1}{4\pi} \int_0^{2\pi} \int_0^\pi |\mathcal{B}(f, \theta, \phi)|^2 \sin \theta \, d\theta \, d\phi} \\ &= \frac{|\mathbf{h}^H(f) \mathbf{d}(f, \theta_d)|^2}{\mathbf{h}^H(f) \mathbf{\Gamma}(f) \mathbf{h}(f)} \end{aligned} \quad (2.17)$$

which is the ratio between the array gain in the look direction  $\theta_d$  and the average gain over all other directions.  $\mathbf{\Gamma}(f)$  is the pseudo-coherence matrix whose elements are

$$[\mathbf{\Gamma}(f)]_{i,j} = \text{sinc} \left( \frac{2\pi f \|\mathbf{r}_i - \mathbf{r}_j\|_2}{c} \right) \quad (2.18)$$

where  $\mathbf{r}_i, \mathbf{r}_j$   $1 \leq i, j \leq N$  are the coordinates of the  $i$  and  $j$  microphones. The broadband DF is defined as

$$\mathcal{D} = \frac{\int_f |\mathbf{h}^H(f) \mathbf{d}(f, \theta_d)|^2 df}{\int_f \mathbf{h}^H(f) \mathbf{\Gamma}(f) \mathbf{h}(f) df}. \quad (2.19)$$

## 2.4 Genetic Algorithms

The genetic algorithm (GA) is an optimization and search technique inspired by the Darwinian theory of evolution, in which only the most adaptive individuals contribute their traits to successive generations. In a GA, a population of potential solutions to a given problem evolves over several generations, driven by a fitness function that evaluates the quality of each candidate solution. Each possible solution is represented by a sequence of genes called chromosomes where the set of solutions is called a population. The population converges toward optimal or near-optimal solutions, through iterative processes involving three fundamental operators:

- **Selection** is the mechanism by which individuals are chosen from the current population to participate in reproduction. The probability of an individual being selected is proportional to its fitness, as measured by the problem's objective function. This ensures that better solutions are more likely to pass on their genetic material to the next generation.
- **Crossover**, is the process of creating offspring by combining the genetic material of two parent solutions. It plays a critical role in exploration by introducing new combinations of genes, potentially leading to superior solutions. Crossover ensures genetic diversity while preserving the essential traits of the parents. Its effectiveness depends on the crossover rate, which determines how often the operation is applied.
- **Mutation** introduces random alterations in the genes of individuals, simulating the biological mutation process. It ensures genetic diversity within the population

and prevents premature convergence to local optima. Mutation is particularly important in maintaining exploration in later generations when the population tends to become homogeneous. The mutation rate, a key parameter, determines how frequently mutation occurs. A low mutation rate helps preserve the structure of promising solutions, while a higher rate ensures continued exploration of the search space.

One of the key strengths of Genetic Algorithms is their ability to effectively solve complex optimization problems across diverse domains. They are highly adaptable and can handle a wide variety of problem types, including non-linear, multi-modal, and high-dimensional optimization problems. GAs do not require gradient information, making them suitable for problems with discontinuous, noisy, or non-differentiable objective functions. Additionally, their stochastic nature allows them to escape local optima, increasing the likelihood of finding global solutions. GAs are also inherently parallelizable, enabling efficient implementations on modern computational architectures. However, GAs have some limitations. They can be computationally expensive, especially for problems with large search spaces or when fitness evaluations are costly. Without careful parameter tuning, such as mutation and crossover rates, they may converge prematurely to suboptimal solutions or require excessive iterations to converge. Furthermore, GAs do not guarantee an optimal solution and may only provide near-optimal results, which might be insufficient for certain critical applications. Despite these drawbacks, GAs remain a versatile and powerful optimization tool in many fields.

## Chapter 3

# Constant Elevation-Beamwidth Beamforming with CRAs

In this chapter, we present a hybrid approach for the design of a CB FIR beamformer with CRAs. The proposed approach optimizes simultaneously the ring radii and the FIR coefficients. This problem is generally nonlinear and nonconvex; however, for fixed radii, the relationship becomes linear and can be solved as a convex problem. Therefore, we decompose the optimization problem into two parts: a global search optimization and a convex one, where the second is incorporated as the cost of the first.

In Section 3.1, we formulate the optimization constraints and objective function regarding the FIR-beamformer coefficients. This optimization problem aims to design a CB beampattern for a given CRA configuration with flexible control of the DF and WNG. Following, in Section 3.2, we incorporate the above optimization problem as the cost of a genetic algorithm.

### 3.1 Constant-Beamwidth Beampattern Design

The following subsections describe the main steps in the CB FIR-beamformer design for a given CRA configuration: In Section 3.1.1, the continuous-phase representation is used to define the optimization problem in terms of the FIR coefficients. Next, the optimization constraints maintaining CB are defined in Section 3.1.2. Finally, in Section 3.1.3, an objective function is suggested that allows a tradeoff between WNG and DF.

#### 3.1.1 Time Domain Filter Design

Implementing a broadband beamformer in the time domain is essential for applications requiring computational efficiency and low latency [41]. The FIR frequency response  $H_m(f)$  is defined as

$$H_m(f) = \sum_{n=0}^L b_{n,m} e^{-j2\pi fn} \quad (3.1)$$

where  $\{b_{n,m}\}_{n=0}^L$  are the real-valued coefficients of the  $m$ -th ring and  $L$  denotes the order of the filter. The design of an FIR filter is done by computing the optimal impulse response coefficients  $\{b_{n,m}\}_{n=0}^L$  concerning a chosen performance measure. In many applications, such as speech, filtering the signal without distortion is desirable. This is why linear phase filters are preferred, as their linear phase characteristic introduces a pure time delay. The frequency response  $H_m(f)$  can be expressed as

$$H_m(f) = A_m(f) e^{j\phi_m(f)} \quad (3.2)$$

where  $A_m(f)$  is a real-valued amplitude function and  $\phi_m(f)$  is continuous phase. This form is called a continuous-phase representation and is very common in filter design.

We design the filters as Type-I linear-phase FIR filters with even order and symmetric coefficients. All filters have the same order to maintain a fixed time delay, so  $\phi_m(f) = 2\pi fL/2$ . Type-I filters are a good choice due to their versatility [42]. Consequently, the amplitude function can be written in the form

$$A_m(f) = \sum_{n=0}^{L/2} \tilde{b}_{n,m} \cos(2\pi fn) \quad (3.3)$$

where

$$\tilde{b}_{n,m} = \begin{cases} b_{L/2,m} & n = 0 \\ 2b_{L/2-n,m} & 1 \leq n \leq L/2. \end{cases} \quad (3.4)$$

Let  $\Phi$  denote the frequency range of interest. We uniformly discretize the frequency space and introduce  $K$  frequency bins  $\{f_k\}_1^K \in \Phi$ . We denote  $\mathbf{b}_m$  as a vector of length  $(L/2 + 1)$  containing the coefficients of the  $m$ -th ring, and  $\mathbf{B}$  as a  $(L/2 + 1) \times M$  matrix containing the coefficients of all rings, that is,

$$\mathbf{b}_m = (b_{0,m}, \dots, b_{L/2,m})^T \quad (3.5)$$

$$\mathbf{B} = (\mathbf{b}_1, \dots, \mathbf{b}_M) . \quad (3.6)$$

We arrange the cosines values at frequency  $f$  in the vector  $\mathbf{g}(f)$  of length  $(L/2 + 1)$ , and the values across all frequency bins in the  $(L/2 + 1) \times K$  matrix  $\mathbf{G}$ , that is,

$$\mathbf{g}(f) = [1, 2 \cos(2\pi f), \dots, 2 \cos(2\pi fL/2)]^T \quad (3.7)$$

$$\mathbf{G} = [\mathbf{g}(f_1), \dots, \mathbf{g}(f_K)] . \quad (3.8)$$

Then, the amplitude function in matrix form, evaluated over the frequency grid, is given by

$$\mathbf{A} = \mathbf{B}^T \mathbf{G} \quad (3.9)$$

where  $\mathbf{A}$  is a  $M \times K$  matrix with entries holding  $(\mathbf{A})_{k,m} = A_m(f_k)$ .

### 3.1.2 Optimization Constraints

We present a set of constraints that should be considered while designing CB beamformers.

The first constraint restricts the FIR coefficients to the class of Type-I FIR filters and the amplitude response to be real-valued:

$$\mathcal{C}_1 : \mathbf{A} = \mathbf{B}^T \mathbf{G}. \quad (3.10)$$

The second is the well-known distortionless response constraint, which ensures that any signal arriving from the desired direction will pass the beamformer without distortion, given by

$$\underline{\mathbf{h}}^T(f_k) \mathbf{T}^T \mathbf{d}(f_k, \theta_d) = 1, \forall f_k \in \Phi \quad (3.11)$$

Since we restrict ourselves to Type-I FIR filters, by (3.2), the filters frequency response can be expressed as

$$\underline{\mathbf{h}}(f_k) = \mathbf{a}_k e^{-j2\pi f L/2} \quad (3.12)$$

where  $\mathbf{a}_k$  denotes the  $k$ -th column of the matrix  $\mathbf{A}$ . All filters share the same continuous linear phase response (pure delay) which by the commutative property of LTI systems can be applied after the summation part in Fig. 2.2, resulting

$$\mathcal{C}_2 : (\mathbf{T} \mathbf{a}_k)^T \mathbf{d}(f_k, \theta_d) = 1, \forall f_k \in \Phi, \quad (3.13)$$

The beamformer aims to maintain CB across a large frequency range. Let  $\Theta_{BW}$ ,  $\Phi_{BW}$  denote the angles and frequencies that cover the mainlobe region, respectively. We define the matrix  $\mathbf{B}^{BW}$  containing the samples of the beampattern power over the grid as

$$\left(\mathbf{B}^{BW}\right)_{k,i} = \mathcal{B}[(\mathbf{T} \mathbf{a}_k), \theta_i] \quad (3.14)$$

where  $k \in [1, |\Phi_{BW}|]$  and  $i \in [1, |\Theta_{BW}|]$ . Hence, a CB can be achieved by restricting the magnitude to be greater or equal to the magnitude at the mainlobe region, expressed as

$$\mathcal{C}_3 : \mathbf{B}^{BW} \geq A_{BW}, \quad (3.15)$$

where  $A_{BW}$  marks the  $-3$  dB amplitude. In addition, the maximal beampattern fluctuation within the mainlobe region is constrained to be less than  $\delta$ , that is,

$$\mathcal{C}_4 : \max \left| \mathbf{B}^{BW} - \mathbf{1}_{|\Phi_{BW}|} \otimes \mathbf{B}_{|\Phi_{BW}|}^{BW} \right| \leq \delta, \quad (3.16)$$

where  $\mathbf{B}_{|\Phi_{BW}|}^{BW}$  is the  $|\Phi_{BW}|$ -th row of  $\mathbf{B}^{BW}$ , i.e., the beampattern of the highest frequency in the mainlobe region serving as a reference beampattern.

Furthermore, to avoid negative amplification values and improve robustness, a fifth

constraint on the amplitude is added:

$$\mathcal{C}_5 : 0 \leq \mathbf{a}_k \leq 1, \forall k \in [1, K]. \quad (3.17)$$

### 3.1.3 Objective Function

Under the distortionless constraint in (3.13), the broadband DF and WNG can be expressed, respectively, as

$$\mathcal{D} = \sum_{k=1}^K \left[ (\mathbf{T}\mathbf{a}_k)^T \mathbf{\Gamma}(f_k) \mathbf{T}\mathbf{a}_k \right]^{-1} \quad (3.18)$$

and

$$\mathcal{W} = \sum_{k=1}^K \left[ (\mathbf{T}\mathbf{a}_k)^T \mathbf{T}\mathbf{a}_k \right]^{-1}. \quad (3.19)$$

We suggest the combination of the two as an objective function for the minimization problem, which is given by

$$\alpha \mathcal{D}^{-1} + (1 - \alpha) \mathcal{W}^{-1} \quad (3.20)$$

where  $\alpha$  is a constant between 0 and 1, controlling the tradeoff between DF and WNG. A bigger  $\alpha$  makes the DF more significant.

To sum up, the CB FIR-beamformer for a given CRA configuration can be derived by solving the following CQP optimization problem:

$$\begin{aligned} \min_{\mathbf{A}, \mathbf{B}} \quad & \alpha \mathcal{D}^{-1} + (1 - \alpha) \mathcal{W}^{-1} \\ \text{s.t.} \quad & \mathcal{C}_1, \mathcal{C}_2, \mathcal{C}_3, \mathcal{C}_4, \mathcal{C}_5. \end{aligned} \quad (3.21)$$

## 3.2 Hybrid Optimization using Genetic Algorithm

GA is a stochastic optimization technique inspired by natural selection, where a population of solutions evolves to solve complex problems efficiently.

In this paper, a candidate solution is a vector  $\mathbf{r} = (R_1, \dots, R_M)^T$  containing  $M$  real-valued ring radii, lying in the interval  $[R_{min}, R_{max}]$ . All solutions are normalized to have values between 0 and 1, and referred to as chromosomes. Without loss of generality, we assume the genes in a chromosome are sorted in ascending order. Next, we describe the main stages of the GA.

### Initial Population

An initial population of chromosomes  $\{\mathbf{x}_i\}_{i=1}^{N_{pop}}$  is generated by

$$\mathbf{x}_i = \mathbf{x}_{un} + \mathbf{n}_i \quad (3.22)$$

where  $\mathbf{x}_{un}$  is the uniform solution of  $N_{genes}$  evenly spaced points in the  $[0, 1]$  interval, and  $\mathbf{n}_i$  is a  $N_{genes} \times 1$  white Gaussian noise vector, with zero mean and standard deviation of  $\sigma_{pop}$ .

### Fitness Calculation

The fitness of a chromosome describes how good is the solution. We use the negative of the cost obtained by the CQP optimization problem defined in (3.21) as the fitness where the fitness of the non-solvable chromosomes is set to the lowest fitness in the population. Next, the fitness values are scaled using the rank-scaled (RS) [43] technique, which scale the fitness values by their rank ordering preventing premature convergence.

### Elitism

To ensure that the best solution won't be lost, we use the elitism strategy by passing the  $N_{elite}$  best chromosomes directly to the next generation.

### Selection

Choosing the most fit parent chromosomes for reproduction is done using the stochastic universal sampling (SUS) [44] technique. In this technique, the chromosomes are chosen by one spinning of a roulette wheel with sections proportional to the fitness values and multiple equally spaced selection points, giving weaker solutions a chance to be chosen.

### Crossover

Every two parents produce a child by combining their genetics using the extended intermediate crossover (EIC) [45] operator. Let  $\mathbf{x}$  and  $\mathbf{y}$  be two parent chromosomes. Then, a child chromosome is produced by

$$\mathbf{z} = \mathbf{x} + \boldsymbol{\alpha} \circ (\mathbf{y} - \mathbf{x}) \quad (3.23)$$

where  $\boldsymbol{\alpha}$  is a random vector with elements uniformly distributed in the  $[-0.25, 1.25]$  interval. The solutions are generated in a slightly larger hypercube, allowing the exploration of new solutions.

### Mutation

Mutation allows the algorithm to explore new solutions and divert from converging to popular solutions. We use the dynamic multi-nonuniform mutation (DMNUM) [46] which decreases the mutation search interval as time progresses. Let  $\mathbf{x}$  be a parent chromosome and  $\mathbf{z}$  the produced child. We first generate a random vector  $\mathbf{p}$  of length  $N_{genes}$  with elements uniformly distributed in the  $[0, 1]$  interval. A gene is chosen to

mutate if its probability is lower than the mutation probability  $p_{mu}^{gene}$ . Next, we iterate in random order over the chosen genes and apply the following mutation operation:

$$z_i = \begin{cases} x_i + [x_{i-1} - x_i] f(g), & w.p. 0.5 \\ x_i - [x_i - x_{i+1}] f(g), & w.p. 0.5 \end{cases} \quad (3.24)$$

$$f(g) = r \left( 1 - \frac{g}{G_{max}} \right)^\gamma \quad (3.25)$$

where  $r$  is a uniform random number in the  $[0, 1]$  interval,  $g$  is the current generation,  $G_{max}$  is the maximum number of generations and  $\gamma$  is a shape parameter. In the boundaries we use  $x_0 = 0$  and  $x_{N_{genes}+1} = 1$ .

The algorithm terminates when the fitness of the fittest member does not change over a certain number of generations or when it reaches the maximal number of generations. To ensure that the individuals meet the constraints, we repair them by clipping and sorting after each operator.

The steps of the hybrid approach CB FIR beamformer are summarized in Algorithm 3.1.

---

**Algorithm 3.1** Hybrid Genetic Algorithm

---

- 1: Generate initial population of size  $N_{pop}$ .
  - 2: **for**  $i = 1$  to  $N_{gen}$  **do**
  - 3:   **for**  $j = 1$  to  $N_{pop}$  **do**
  - 4:     Evaluate fitness by solving (3.21).
  - 5:   **end for**
  - 6:   Scale fitness with RS.
  - 7:   **if** convergence satisfied **then**
  - 8:     break.
  - 9:   **end if**
  - 10:   Transfer  $N_{elite}$  best individuals to next generation.
  - 11:   Select  $2(N_{pop} - N_{elite})$  individuals with SUS.
  - 12:   **for**  $j = 1$  to  $(N_{pop} - N_{elite})$  **do**
  - 13:     Apply EIC (3.23).
  - 14:     Apply DMNUM (3.24) w.p.  $p_{mu}$ .
  - 15:     Repair individuals.
  - 16:   **end for**
  - 17:   Replace the old population with the next generation.
  - 18: **end for**
  - 19: **return** best individual.
-

### 3.3 Experimental Results

In this section, we provide a few simulation results examining the performance of the proposed approach compared to the state-of-the-art approach suggested by Kleiman [40]. In sections 3.3.1 to 3.3.3, the simulations demonstrate the advantages of the proposed CQP optimization for designing CB beamformers for a given CRA configuration. In Section 3.3.4, the simulations show the hybrid approach's advantage in computation time.

All simulations consider the design of a CB beampattern obtaining a beamwidth of  $\theta_{BW} = 30^\circ$  measured at amplitude  $A_{BW} = 1/\sqrt{2}$  over the range of frequencies  $[0, 8]$  kHz. The DoA of the desired signal is  $\theta_d = 0$ . The optimization problems were implemented in MATLAB using the CVX toolbox [47] and the MOSEK solver, and conducted on a Xeon E5-2697V4 CPU @ 2.3 GHz of Intel with 128GB of RAM. The source code for this paper can be found at. <sup>1</sup>

In sections 3.3.1 to 3.3.3, we consider the design of a CB FIR beamformer for a given CRA configuration. The chosen CRA configuration is a non-uniform CRA consisting of  $M = 5$  rings, with radii  $R_m = (2, 4.8, 8.1, 13.9, 25)^T$  cm, containing  $N_m = (6, 15, 17, 19, 19)^T$  microphones, the same as that of Kleiman [40].

#### 3.3.1 Influence of $\alpha$

The beampatterns power as a function of frequency and elevation for  $\alpha = 1, 0.3, 0$  and  $L = 32$  are shown in Figures 3.1(a)-(c), respectively. The overlaid dashed line is the half-power of the mainlobe. We can observe that the beamwidth is constant over the entire desired frequency range  $\Phi_{BW} = [1.2, 8]$  kHz and mainlobe region  $\Theta_{BW} = [-15^\circ, 15^\circ]$ . The beamformer weights as a function of frequency applied to the rings for  $\alpha = 1, 0.3, 0$  and  $L = 32$  are shown in Figures 3.1(d)-(f), respectively. The choice of  $\alpha = 1$ , shown in Figures 3.1(a),(d), yields the maximum DF CB beamformer. We can see that the sidelobe level is low compared to the others, which is desired to reduce diffuse noise. Moreover, the produced filters are band-pass in nature. As the frequency increases, the inner rings dominate, while the outer ones become less dominant. The choice of  $\alpha = 0$ , shown in Figures 3.1(c),(f), yields the delay-and-sum CB beamformer. The produced filters are low-pass in nature. As the frequency decreases, more rings participate in the beamforming process, which can be thought of as beamforming with discrete pistons. In the low-frequency region, all the rings are active, which is desirable for reducing the microphone's inner white noise. For the choice of  $\alpha = 0.3$ , shown in Figures 3.1(b),(e), we get a compromise between the two beamformers above. The produced filters are band-pass in nature, with more extensive support toward the low frequencies, increasing the number of microphones participating in the beamforming process and reducing the microphone's inner white noise. For more on the tradeoff

---

<sup>1</sup><https://github.com/PeretzOrel/CB-EL-CRA>

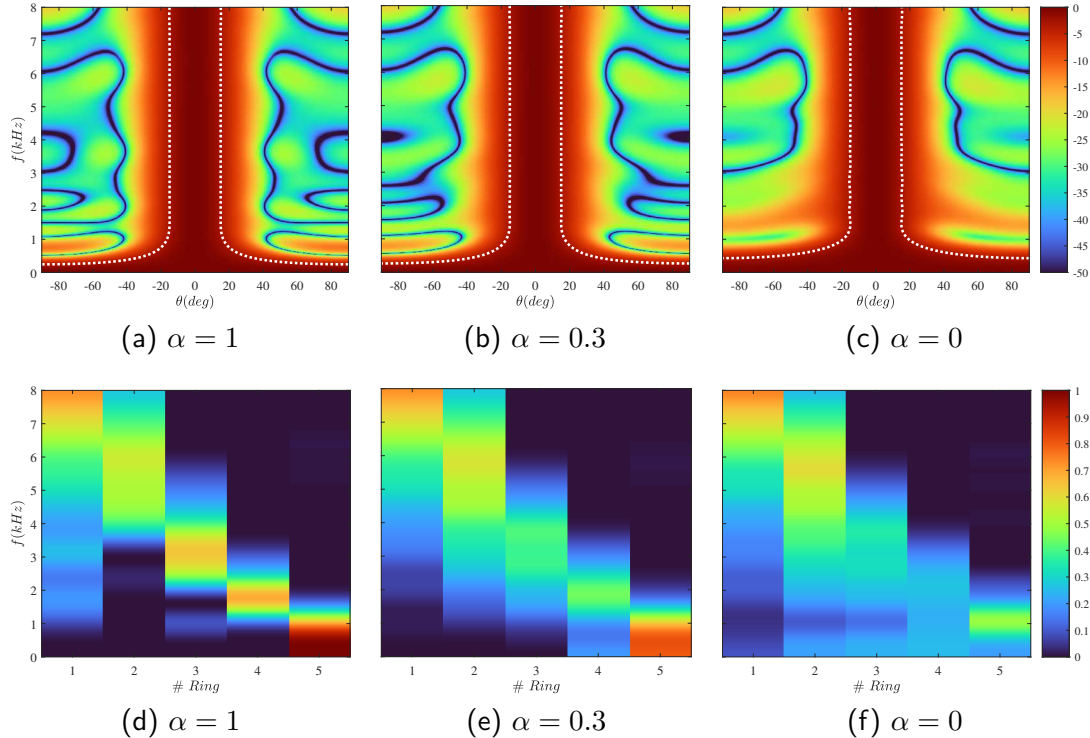


Figure 3.1: (a-c) Beampatterns of the proposed beamformer for a non-uniform CRA with  $M = 5$  rings and  $L = 32$  filter taps. The overlaid dashed line is the half-power contour of the mainlobe. (d-f) Weight values are applied to the rings at each frequency.

between beamwidth, radii, and frequency using discrete rings and pistons, the reader is referred to [33]. Overall, the definition of a single optimization problem, optimizing the FIR coefficients of all rings jointly, has several advantages. First, the design process is straightforward, produces smooth and continuous FIR filter responses, and does not require a pre-processing step, as suggested in Kleiman [40]. Second, the filter weights of different rings are dependent, and the ripples are coordinated, resulting in better beamwidth consistency, as shown in the following subsections.

Figures 3.2(a)–(b) show the DF and WNG as a function of frequency obtained by Kleiman [40] and the proposed approach for  $\alpha = 1, 0.3, 0.15, 0$  and  $L = 32$ . The choice of  $\alpha = 1$  yields the maximum DF CB beamformer, which maximizes the DF. The proposed beamformer attains slightly higher DF and WNG for most frequencies due to the direct and joint filter design. For the choice of  $\alpha = 0$ , we get the delay-and-sum CB beamformer, which maximizes the WNG. The suggested objective function allows a tradeoff between WNG and DF, which can be observed for  $\alpha = 0.15, 0.3$ . A bigger  $\alpha$  improves the DF at the expense of the WNG. One can see that the choice of  $\alpha = 0.3$  can be picked as a good compromise between WNG and DF. By allowing a maximal reduction of 0.5 dB in the DF, we improve the WNG by more than 1 dB in the low-frequency region and a maximal improvement of about 3dB at  $f = 1.8$  kHz.

Figure 3.2(c) illustrates the beamwidth as a function of frequency obtained by

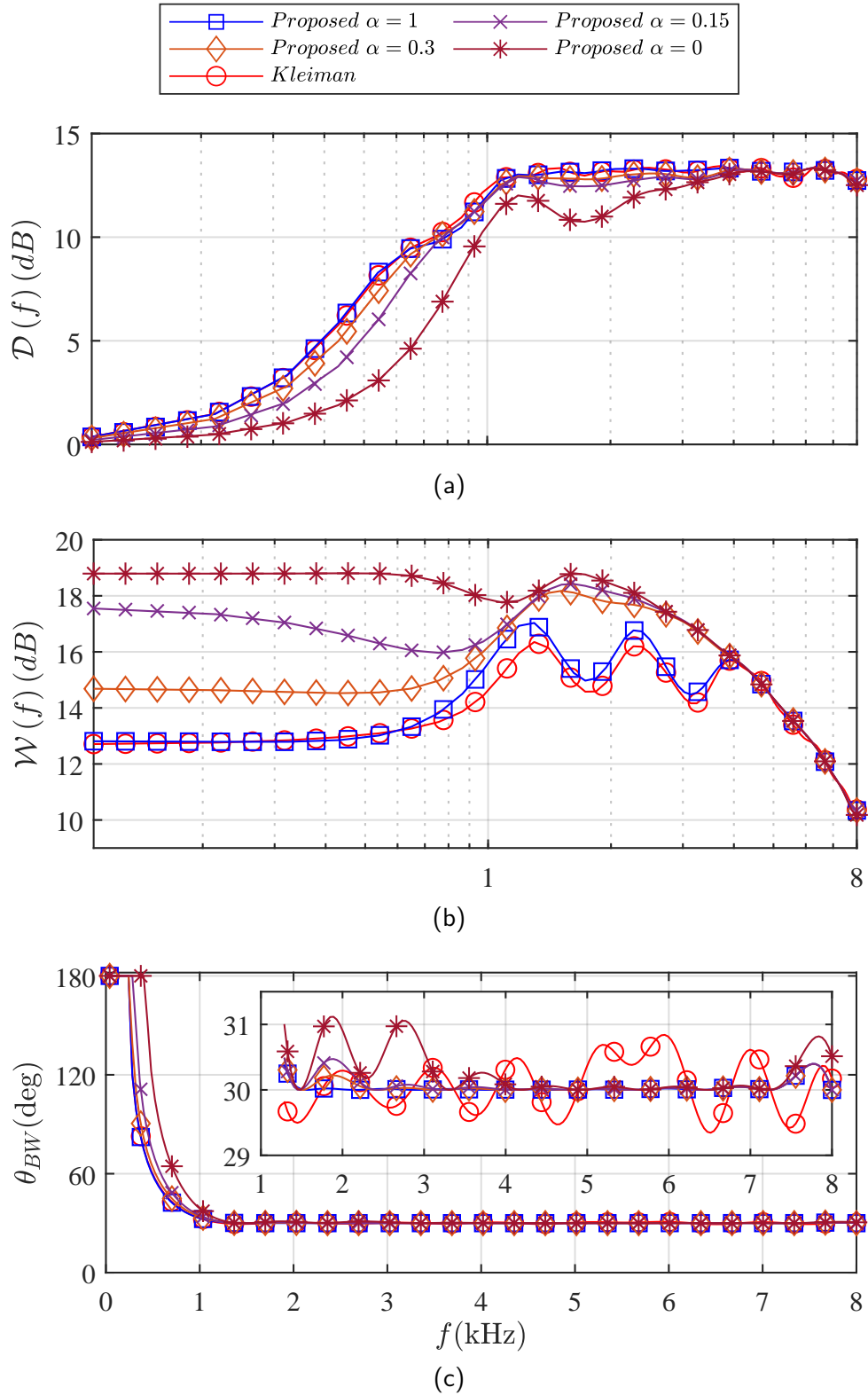


Figure 3.2: Performance measures of the proposed beamformer with  $\alpha = 1$  (square),  $\alpha = 0.3$  (diamond),  $\alpha = 0.15$  (cross),  $\alpha = 0$  (asterisk), and Kleiman [40] (circle) for  $L = 32$  filter taps. (a) DF, (b) WNG, and (c) Beamwidth  $\theta_{BW}$ , as a function of frequency.

Kleiman [40] and the proposed approach for  $\alpha = 1, 0.3, 0.15, 0$  and  $L = 32$ . The mean and standard deviation of the beamwidth can measure the beamwidth consistency. Both approaches maintain an approximately CB of about  $30^\circ$  over the desired frequency range [1.2, 8] kHz. Kleiman’s approach [40] has high ripples that break the constraint of the beamwidth (to be larger than  $\theta_{BW} = 30^\circ$ ) while the proposed approach has low ripples and holds the constraints. The proposed approach obtains better beamwidth consistency due to the direct and joint design of the FIR coefficients.

### 3.3.2 Influence of $L$

The DF, WNG, and beamwidth as a function of frequency obtained by Kleiman [40] and the proposed beamformer for  $\alpha = 1, 0.3, 0.15, 0$  and  $L = 20$  are shown in Fig. 3.3. Compared to the results of  $L = 32$  shown in Fig. 3.2, we notice that a smaller  $L$  damages the flexibility of the proposed approach. The maximal gain in the low-frequency region is reduced to maintain the constant beamwidth constraint. In addition, both approaches have higher ripples.

### 3.3.3 Sidelobe Level Comparison

The sidelobe level is another important performance measure. A beamformer with a low sidelobe level can suppress interference better. The beampatterns at different frequencies in the range of [1.4, 7.6] kHz obtained by the proposed beamformer with  $\alpha = 1$  and Kleiman’s approach [40] for  $L = 32$  are shown in Fig. 3.4. The solid line marks the sidelobe level. The SLL of the proposed approach is  $-22.2$  dB, which is lower by more than 3 dB than Kleiman’s SLL, which is  $-18.6$  dB.

Table 3.1 summarizes the above performance measures for the different parameters. The SLL, beamwidth mean, and standard deviation were measured over [1.4, 7.6] kHz. We can notice the tradeoff between the DF and WNG, controlled by  $\alpha$ . A bigger  $\alpha$  makes the DF more significant, and vice versa. In addition, the proposed approach has better beamwidth consistency (lower standard deviation) for the same number of filter taps. In general, the proposed approach achieves better performance with fewer filter taps.

### 3.3.4 Hybrid Approach

This section considers the joint design of both the beamformer coefficient and the ring radii.

The allowed radii lie between  $R_{min} = 0$  cm and  $R_{max} = 25$  cm. The population size is set to  $N_{pop} = 100$ , and the number of elite individuals to  $N_{elite} = 0.1N_{pop}$ . In each generation, we apply the crossover operation over  $2(N_{pop} - N_{elite})$  individuals. The mutation operation is applied to the offspring with a probability  $p_{mu} = 0.2$ . The Gaussian noise standard deviation used for the initial population generation is  $(R_{max} - R_{min})/5(M - 1)$ . The parameters of DMNUM [46] are  $\gamma = 2$  for the shape parameter,

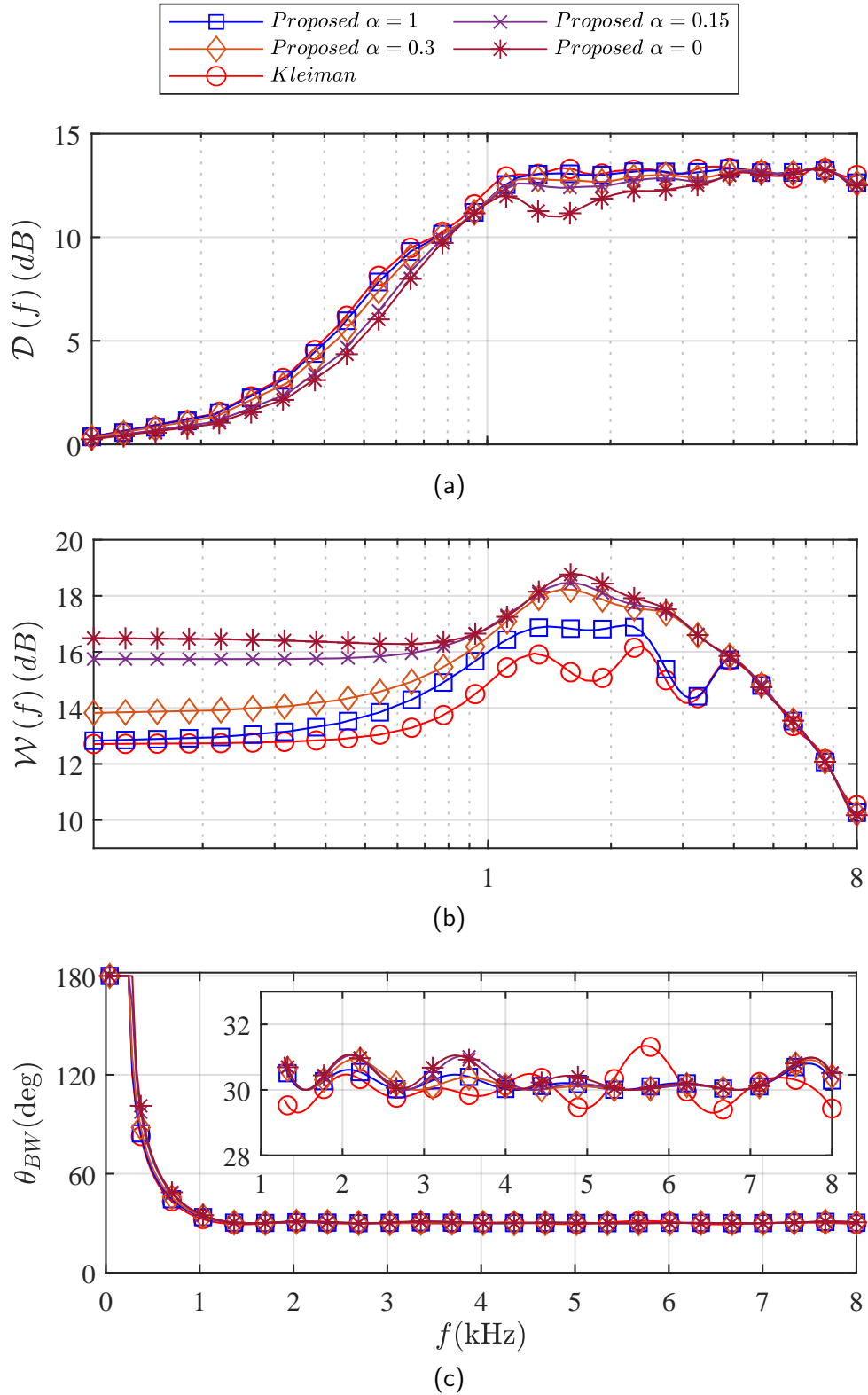


Figure 3.3: Performance measures of the proposed beamformer with  $\alpha = 1$  (square),  $\alpha = 0.3$  (diamond),  $\alpha = 0.15$  (cross),  $\alpha = 0$  (asterisk), and Kleiman [40] (circle) for  $L = 20$  filter taps. (a) DF, (b) WNG, and (c) Beamwidth  $\theta_{BW}$ , as a function of frequency.

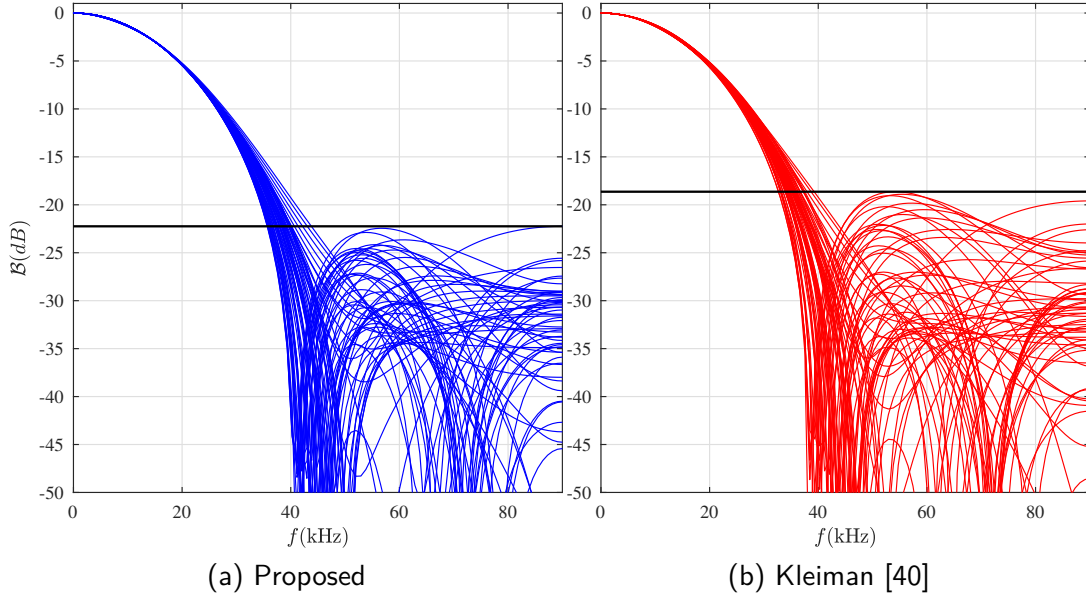


Figure 3.4: Beam patterns at different frequencies in range  $[1.4, 7.6]$  kHz with  $L = 32, \alpha = 1$ . The solid line marks the sidelobe level.

$p_{mu}^{gene} = 0.2$  for the mutation probability of the genes, and  $N_{gen} = 100$  for the maximal number of generations. The cost function of the individuals is evaluated in parallel using the MATLAB parallel toolbox.

Figures 3.5(a)–(b) show the DF and WNG of the proposed hybrid approach as a function of frequency for  $\alpha = 1, 0.3, 0.15, 0$  and  $L = 32$ . For each  $\alpha$  we get different ring radii and weights optimizing the cost objective in (3.21). The produced solutions are summarized in Table 3.2. As  $\alpha$  increases the broadband WNG in (3.21) becomes more dominant and the algorithm prefers weights with larger support resulting by (2.3) more elements in each ring which reduces the inner white noise of the microphones. Compared to Fig. 3.2 where the ring radii and number of microphones per ring were fixed, we get DF and WNG with higher dynamic range resulting from the optimization of the ring radii.

Figure 3.5(c) illustrates the beamwidth as a function of frequency obtained by the proposed hybrid approach for  $\alpha = 1, 0.3, 0.15, 0$  and  $L = 32$ . The proposed hybrid approach maintains an approximately CB of about  $30^\circ$  over the desired frequency range  $[1.2, 8]$  kHz for all  $\alpha$  values.

Figure 3.6 illustrates the algorithm convergence, i.e., the cost value as a function of the generation number obtained by the proposed hybrid approach for  $L = 32$  and  $\alpha = 1$ . The solid line and the shaded area are the mean and standard deviation of the cost over 100 independent MC runs, respectively. As the number of generations increases, the cost value converges to 7 dB with higher confidence. The best solution produced by a random run is  $(2, 4.6, 7.4, 13.5, 25)$  cm, which is quite similar to the solution produced by Kleiman [40]. The average computation time of a single generation is 22 seconds,

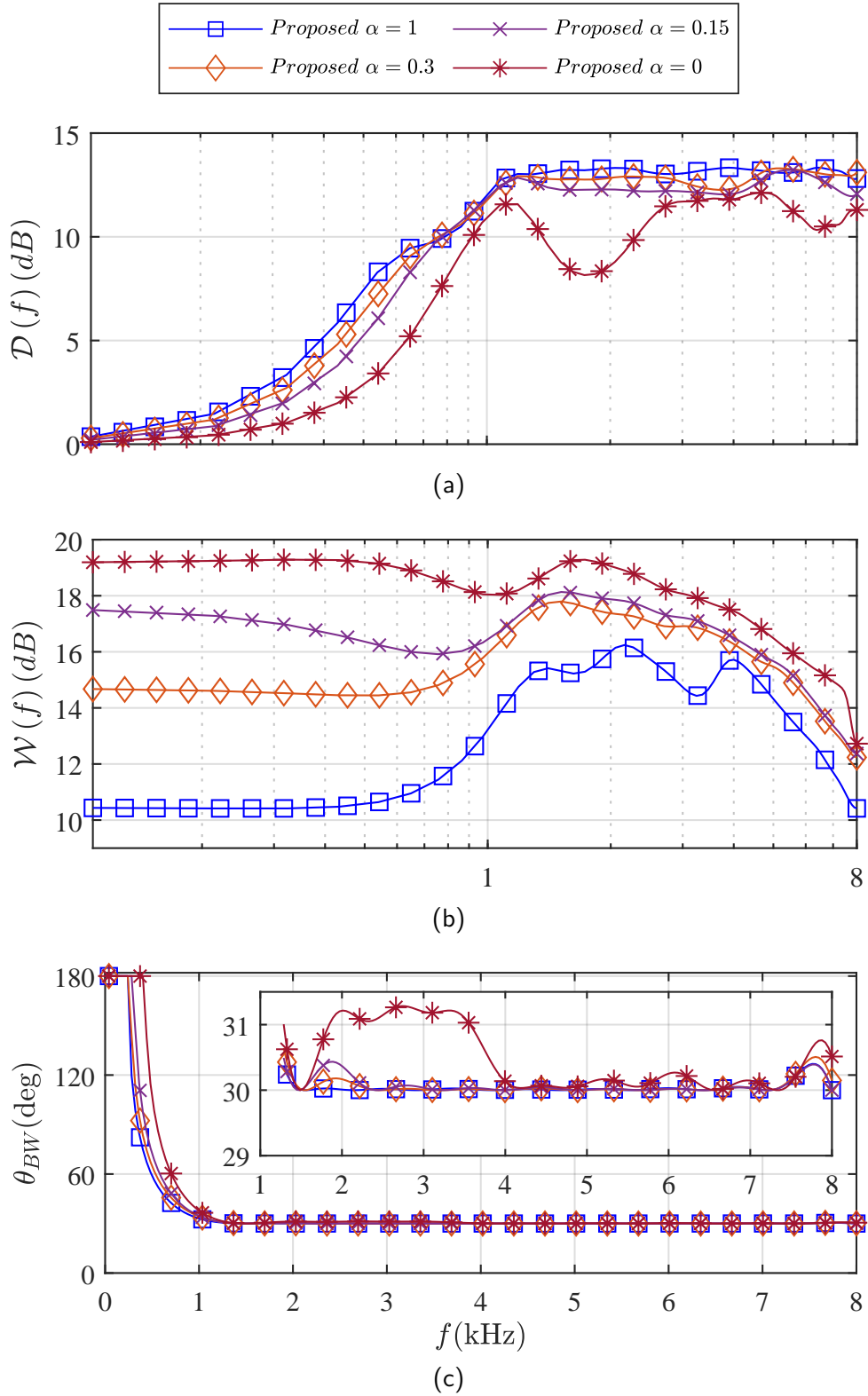


Figure 3.5: Performance measures of the proposed hybrid approach with  $\alpha = 1$  (square),  $\alpha = 0.3$  (diamond),  $\alpha = 0.15$  (cross) and  $\alpha = 0$  (asterisk) for  $L = 32$  filter taps. (a) DF, (b) WNG, and (c) Beamwidth  $\theta_{BW}$ , as a function of frequency.

Table 3.1: Performance measures comparison for different parameter choices

Approach	$L$	$\alpha$	$\mathcal{D}$ (dB)	$\mathcal{W}$ (dB)	$MEAN\{\theta^{\circ}_{BW}\}$	$STD\{\theta^{\circ}_{BW}\}$	$SLL$ (dB)
Proposed	20	1	12.7	14.6	30.2	0.18	-23.7
	20	0.3	12.6	15.3	30.2	0.24	-22.3
	20	0.15	12.5	15.6	30.3	0.34	-20.1
	20	0	12.2	15.7	30.4	0.34	-13.7
	32	1	12.7	14.4	30.02	0.05	-22.2
	32	0.3	12.6	15.3	30.03	0.08	-22.4
	32	0.15	12.5	15.7	30.05	0.09	-21
	32	0	12.1	16.2	30.2	0.3	-14.3
Kleiman [40]	20	-	12.7	14.1	30.08	0.48	-19
	32	-	12.7	14.1	30.06	0.4	-18.6

 Table 3.2: Produced solutions of the hybrid approach for different  $\alpha$  choices

$\alpha$	$R_m$	$N_m$
1	$(2, 4.7, 7.9, 14.7, 25)^T$	$(6, 14, 18, 18, 11)^T$
0.3	$(1.7, 3.7, 6.2, 13, 24.5)^T$	$(6, 12, 17, 20, 19)^T$
0.15	$(2, 3.7, 6.1, 13, 24.8)^T$	$(7, 12, 17, 20, 20)^T$
0	$(2, 3.4, 3.7, 8.8, 23.8)^T$	$(7, 11, 12, 27, 28)^T$

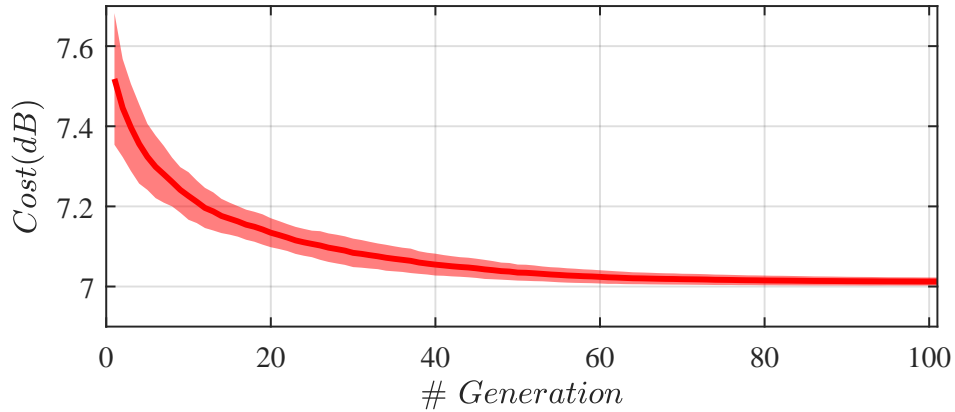


Figure 3.6: Convergence plot. Cost value versus the number of generations obtained by the proposed hybrid approach. The solid line and the shaded area are the mean and standard deviation of the cost over 100 MC runs, respectively.

and for a whole run, it is 36 minutes. While the proposed hybrid approach takes about 36 minutes to run, Kleiman [40] runs for about 8 hours, almost two orders of magnitude more than the proposed approach. If a specific cost value is satisfactory, the proposed approach can stop before  $N_{gen}$ , resulting in a faster runtime.



## Chapter 4

# Conclusions

### 4.1 Summary

In this thesis, we have addressed the problem of constant elevation-beamwidth beamformers design with CRA. In many 3D broadband applications such as audio communication, hearing aids, and radar, constant beamwidth beamforming is needed to prevent signal distortion when the DOA is inaccurate. Among the array geometries, the circular array is favored due to superior performance and 360° azimuth coverage. However, in most existing approaches the DOA is restricted to the horizontal plane and suffers from high computational complexity, especially for large arrays. In this thesis, we have adopted the CRA configuration in which the summation of all signals captured by each microphone in a ring precedes sampling. The beamformer weights were implemented in the time domain using FIR filters. While eliminating beam steering ability, the proposed design requires fewer resources and simplifies the computational complexity. Such an array can be installed as a circular ceiling array over the different regions of interest in applications involving large spaces with distributed speakers. This solution benefits from low cost, latency, and high performance.

In Chapter 3, we introduced a hybrid approach for designing a CB FIR beamformer with CRAs. First, we assumed a CRA with pre-defined radii. In the proposed methodology, a CQP optimization is defined. Multiple constraints are suggested for shaping the array response, maintaining CB over an extensive range of frequencies, and a distortionless response in the DOA of the signal. We utilized the continuous-phase representation of FIR filters, enabling the joint and direct optimization of the time domain FIR coefficients. The objective function includes a control variable, allowing a tradeoff between DF and WNG. Following, a hybrid approach was proposed to optimize the ring radii with a genetic algorithm utilizing the aforementioned convex problem as its cost, exploiting the partial convexity of the problem. The design exploits the degrees of freedom of the array geometry for superior performance. In particular, the ring radii and the beamformer coefficients are optimized simultaneously for all frequencies. Simulation results show that the proposed approach provides a flexible solution for a

good compromise between WNG and DF. In addition, it demonstrates improved performance in WNG, SLL, and beamwidth consistency with reasonable computational complexity.

## 4.2 Future Research

Throughout this thesis, we developed a methodology for an efficient design of a constant elevation-beamwidth beamformer on CRAs. Although superior performance was obtained, as reflected from the simulations, there are still other issues for future research directions that can be conducted:

1. In this work, the number of beamformer weights equals the number of rings, resulting in reduced computational complexity. However, for large CRA with many rings, the computational complexity may still be too high. One possible solution is using a clustered CRA, where the CRA rings are divided into groups that share the same weight. In this case, the joint optimization of the ring radii, the cluster partitions, and the cluster weights should be defined.
2. Volumetric arrays allow sensors to be positioned not only in a 2D plane but also within a 3D volume. These configurations offer additional degrees of freedom, enabling potentially superior performance with respect to 2D arrays. Hence, such an extension should be considered.
3. When deriving the beamformer, several assumptions were made. First, we assumed all microphones were omnidirectional. Using both omnidirectional and directional microphones may improve the array's directivity and enable steering ability. Next, a uniform distance between two adjacent microphones in a ring was considered. Optimizing the number of sensors and their locations inside the rings may lower the number of hardware resources.
4. In real indoor scenarios, the isotropic free space assumption may not hold, and reverberations from the surroundings may degrade severely the performance. Thus, more sophisticated adaptive filtering techniques should be developed.

# Bibliography

- [1] B. Van Veen and K. Buckley, “Beamforming: A versatile approach to spatial filtering,” *IEEE ASSP Mag.*, vol. 5, no. 2, pp. 4–24, Apr. 1988.
- [2] H. L. Van Trees, *Optimum Array Processing: Part IV of Detection, Estimation, and Modulation Theory*. New York, NY, USA: Wiley, 2002.
- [3] J. Benesty, I. Cohen, and J. Chen, *Fundamentals of Signal Enhancement and Array Signal Processing*. Hoboken, NJ, USA: Wiley, 2018.
- [4] M. Brandstein, D. Ward, A. Lacroix, and A. Venetsanopoulos, Eds., *Microphone Arrays: Signal Processing Techniques and Applications*, en. Berlin, Germany: Springer, 2001.
- [5] I. Cohen, J. Benesty, S. Gannot, J. Benesty, and W. Kellermann, Eds., *Speech Processing in Modern Communication: Challenges and Perspectives*, en. New York, NY, USA: Springer, 2010.
- [6] W. Liu and S. Weiss, “New class of broadband arrays with frequency invariant beam patterns,” in *Proc. IEEE Int. Conf. Acoust., Speech, Signal Process.*, vol. 2, Montreal, QC, Canada, 2004, pp. ii–185–188.
- [7] O. Rosen, I. Cohen, and D. Malah, “FIR-based symmetrical acoustic beamformer with a constant beamwidth,” *Signal Process.*, vol. 130, pp. 365–376, 2017.
- [8] Y. Buchris, A. Amar, J. Benesty, and I. Cohen, “Incoherent Synthesis of Sparse Arrays for Frequency-Invariant Beamforming,” *IEEE/ACM Trans. Audio, Speech, Lang. Process.*, vol. 27, no. 3, pp. 482–495, Mar. 2019.
- [9] T. Long, I. Cohen, B. Berdugo, Y. Yang, and J. Chen, “Window-Based Constant Beamwidth Beamformer,” en, *Sensors*, vol. 19, no. 9, p. 2091, May 2019.
- [10] A. Frank and I. Cohen, “Constant-Beamwidth Kronecker Product Beamforming With Nonuniform Planar Arrays,” *Frontiers in Signal Process.*, vol. 2, 2022.
- [11] W. Liu, “Design and implementation of a rectangular frequency invariant beamformer with a full azimuth angle coverage,” *J. of the Franklin Inst.*, vol. 348, no. 9, pp. 2556–2569, Nov. 2011.
- [12] G. Itzhak, I. Cohen, and J. Benesty, “Robust Differential Beamforming with Rectangular Arrays,” en, in *Proc. 29th Eur. Signal Process. Conf.*, Dublin, Ireland, Aug. 2021, pp. 246–250.

- [13] A. Frank, A. Ben-Kish, and I. Cohen, “Constant-Beamwidth Linearly Constrained Minimum Variance Beamformer,” in *Proc. 30th Eur. Signal Process. Conf.*, Aug. 2022, pp. 50–54.
- [14] G. Itzhak and I. Cohen, “Differential and Constant-Beamwidth Beamforming with Uniform Rectangular Arrays,” in *Proc. Int. Workshop Acoust. Signal Enhancement*, Sep. 2022, pp. 1–5.
- [15] G. Itzhak, J. Benesty, and I. Cohen, “Multistage approach for steerable differential beamforming with rectangular arrays,” in *Speech Communication*, vol. 142, pp. 61–76, Jul. 2022.
- [16] V. P. Curtarelli and I. Cohen, “Constant-Beamwidth LCMV Beamformer with Rectangular Arrays,” in *Algorithms*, vol. 16, no. 8, p. 385, Aug. 2023.
- [17] G. Itzhak and I. Cohen, “Region-of-Interest Oriented Constant-Beamwidth Beamforming with Rectangular Arrays,” in *Proc. IEEE Workshop Appl. Signal Proc. Audio Acoust.*, Oct. 2023, pp. 1–5.
- [18] J. Benesty, J. Chen, and I. Cohen, *Design of Circular Differential Microphone Arrays*, in. Berlin, Germany: Springer-Verlag, 2015.
- [19] Y. Wang and Y. Yang, “A Flexible Method for Designing Frequency-Invariant Beamformers With Circular Sensor Arrays,” *IEEE Access*, vol. 6, pp. 57 073–57 084, 2018.
- [20] Y. Buchris, I. Cohen, and J. Benesty, “Frequency-Domain Design of Asymmetric Circular Differential Microphone Arrays,” *IEEE/ACM Trans. Audio, Speech, Lang. Process.*, vol. 26, no. 4, pp. 760–773, Apr. 2018.
- [21] S. C. Chan and H. H. Chen, “Uniform Concentric Circular Arrays With Frequency-Invariant Characteristic - Theory, Design, Adaptive Beamforming and DOA Estimation,” *IEEE Trans. Signal Process.*, vol. 55, no. 1, pp. 165–177, Jan. 2007.
- [22] W. Wang and S. Yan, “A flexible frequency-invariant beampattern synthesis method for concentric circular microphone arrays,” in *Proc. IEEE Int. Conf. Acoust., Speech Signal Process.*, Sep. 2019, pp. 1–6.
- [23] Y. Buchris, I. Cohen, J. Benesty, and A. Amar, “Joint Sparse Concentric Array Design for Frequency and Rotationally Invariant Beampattern,” *IEEE/ACM Trans. Audio, Speech, Lang. Process.*, vol. 28, pp. 1143–1158, 2020.
- [24] Y. Buchris, I. Cohen, and A. Amar, “Design of Frequency-Invariant Beamformers with Sparse Concentric Circular Arrays,” in *Proc. IEEE Workshop Appl. Signal Proc. Audio Acoust.*, Oct. 2023, pp. 1–5.
- [25] H. H. Chen, S. C. Chan, Z. G. Zhang, and K. L. Ho, “Adaptive Beamforming and Recursive DOA Estimation Using Frequency-Invariant Uniform Concentric Spherical Arrays,” *IEEE Trans. Circuits Syst. I: Regular Papers*, vol. 55, no. 10, pp. 3077–3089, Nov. 2008.

- [26] G. Itzhak and I. Cohen, “Differential constant-beamwidth beamforming with cube arrays,” *Speech Communication*, vol. 149, pp. 98–107, 2023.
- [27] G. Huang, J. Benesty, J. Chen, and I. Cohen, “Robust and steerable kronecker product differential beamforming with rectangular microphone arrays,” en, in *Proc. IEEE Int. Conf. Acoust., Speech Signal Process.*, 2020, pp. 211–215.
- [28] C. Mathews and M. Zoltowski, “Eigenstructure techniques for 2-D angle estimation with uniform circular arrays,” *IEEE Trans. Signal Process.*, vol. 42, no. 9, pp. 2395–2407, Sep. 1994.
- [29] M. I. Dessouky, H. Sharshar, and Y. Albagory, “Efficient Sidelobe Reduction Technique for Small-Sized Concentric Circular Arrays,” *Prog. Electromagnetics Res.*, vol. 65, pp. 187–200, 2006.
- [30] H. H. Chen, S. C. Chan, and K. L. Ho, “Adaptive Beamforming Using Frequency Invariant Uniform Concentric Circular Arrays,” *IEEE Trans. Circuits Syst. I: Regular Papers*, vol. 54, no. 9, pp. 1938–1949, Sep. 2007.
- [31] G. Huang, J. Chen, and J. Benesty, “Insights Into Frequency-Invariant Beamforming With Concentric Circular Microphone Arrays,” *IEEE/ACM Trans. Audio, Speech, Lang. Process.*, vol. 26, no. 12, pp. 2305–2318, Dec. 2018.
- [32] R. Sharma, I. Cohen, and B. Berdugo, “Controlling Elevation and Azimuth Beamwidths With Concentric Circular Microphone Arrays,” *IEEE/ACM Trans. Audio, Speech, Lang. Process.*, vol. 29, pp. 1491–1502, 2021.
- [33] A. Kleiman, I. Cohen, and B. Berdugo, “Constant-Beamwidth Beamforming with Concentric Ring Arrays,” en, *Sensors*, vol. 21, no. 21, p. 7253, Jan. 2021.
- [34] E. I. Elsaydy, M. I. Dessouky, S. Khamis, and Y. Albagory, “Concentric Circular Antenna Array Synthesis Using Comprehensive Learning Particle Swarm Optimizer,” *Prog. Electromagnetics Res. Letters*, vol. 29, pp. 1–13, 2012.
- [35] M. Carlin, G. Oliveri, and A. Massa, “Hybrid BCS-Deterministic Approach for Sparse Concentric Ring Isophoric Arrays,” *IEEE Trans. Antennas Propag.*, vol. 63, no. 1, pp. 378–383, Jan. 2015.
- [36] D. Jamunaa, G. Mahanti, and F. N. Hasoon, “Optimized inter-element arc spacing and ring radius in the synthesis of phase-only reconfigurable concentric circular array antenna using various evolutionary algorithms,” en, *Electromagnetics*, vol. 40, no. 2, pp. 104–118, Feb. 2020.
- [37] O. M. Bucci and D. Pinchera, “A Generalized Hybrid Approach for the Synthesis of Uniform Amplitude Pencil Beam Ring-Arrays,” *IEEE Trans. Antennas Propag.*, vol. 60, no. 1, pp. 174–183, Jan. 2012.
- [38] X. Zhao, Q. Yang, and Y. Zhang, “A Hybrid Method for the Optimal Synthesis of 3-D Patterns of Sparse Concentric Ring Arrays,” *IEEE Trans. Antennas Propag.*, vol. 64, no. 2, pp. 515–524, Feb. 2016.

- [39] J. Yang, F. Yang, P. Yang, and Z. Xing, “Synthesis of Clustered Concentric Ring Arrays Through Joint Optimization of Multi-Parameters,” *IEEE Trans. Antennas Propag.*, vol. 71, no. 1, pp. 840–851, Jan. 2023.
- [40] A. Kleiman, I. Cohen, and B. Berdugo, “Constant-Beamwidth Beamforming With Nonuniform Concentric Ring Arrays,” *IEEE/ACM Trans. Audio, Speech, Lang. Process.*, vol. 30, pp. 1952–1962, 2022.
- [41] L. C. Godara, “Application of the Fast Fourier Transform to Broadband Beamforming,” *The Journal of the Acoustical Society of America*, vol. 98, no. 1, pp. 230–240, Jul. 1995.
- [42] B. Porat, *A Course in Digital Signal Processing*, en. New York: Wiley, 1997.
- [43] J. E. Baker, “Adaptive Selection Methods for Genetic Algorithms,” in *Proc. 1st Int. Conf. Genetic Algorithms*, USA: L. Erlbaum Associates Inc., Jul. 1985, pp. 101–111.
- [44] J. E. Baker, “Reducing Bias and Inefficiency in the Selection Algorithm,” in *Proc. 2nd Int. Conf. Genetic Algorithms*, USA: L. Erlbaum Associates Inc., Oct. 1987, pp. 14–21.
- [45] H. Mühlenbein and D. Schlierkamp-Voosen, “Predictive Models for the Breeder Genetic Algorithm I. Continuous Parameter Optimization,” *Evolutionary Computation*, vol. 1, no. 1, pp. 25–49, Mar. 1993.
- [46] J. Yang, P. Yang, F. Yang, and Z. Xing, “A Hybrid Approach for the Synthesis of Nonuniformly Spaced and Excited Linear Arrays With Strict Element Spacing Constraints,” *IEEE Trans. Antennas Propag.*, vol. 70, no. 7, pp. 5521–5533, Jul. 2022.
- [47] M. Grant and S. Boyd, *CVX: Matlab Software for Disciplined Convex Programming, version 2.1*, 2014.

בין מדד הכיווניות לבין מדד הגבר הרעש הלבן (גמישות לתכנון מעצבי אלומה שונים). לאחר מכן, מוצעת שיטה היברידית לאופטימיזציה של רדיוסי הטבעות באמצעות אלגוריתם גנטי, תוך שימוש בבעיה הקמורה שהוזכרה כפונקציית העלות של האלגוריתם הגנטי, ובכך מנצלת בצורה חכמה את הקמירות החלקית של הבעיה. התכן מנצל את דרגות החופש של גאומטריית המערך להשגת ביצועים טובים יותר. בפרט, רדיוסי הטבעות ומקדמי מעצב האלומה מותאמים בו-זמנית עבור כל התדרים. תוצאות ניסוי מדגימות את הגמישות והיתרונות של הגישה המוצעת בהשוואה לפתרונות העדכניים ביותר במונחים של גורם כיווניות, הגבר רעש לבן, רמת אינות צד ועקביות רוחב האלומה, תוך שימוש במשאבים מופחתים וזמן חישוב נמוך משמעותית.

## תקציר

עיצוב אלומה היא שיטה קלאסית חשובה לסינון מרחבי של אות רצוי מתוך רעש והפרעות סביבתיות, תוך שימוש בתצפיות ממספר מיקרופונים. על ידי החלת השהיות ומשקלים מתאימים על אותות המיקרופונים, ניתן לכוון את המערך במרחב ולהתמקד במקור הקול הרצוי. סינון כיווני זה משפר משמעותית את איכות האות ואת מובנות הדיבור, מה שהופך את מעצב האלומה לרכיב חיוני במערכות שמע ותקשורת רבות. השיטה אומצה באופן נרחב ביישומים כמו טלפוניה ללא ידיים, מכשירי שמיעה, מערכות ועידה חכמות, מערכות מגלה כיוון מרחק (מכ"מ) ועוד. בתרחישים מציאותיים, האותות הם לרוב רחבי סרט ובסביבה תלת-ממדית מורכבת, דבר שדורש פתרונות יעילים המשיגים ביצועים גבוהים, השהיה נמוכה ושימוש מינימלי במשאבים.

עיצוב אלומה קונבנציונלי סובל מכך שרוחב האלומה הולך ונעשה צר יותר ככל שהתדר עולה. אותות רחבי סרט שמגיעים מכיוונים השונים מכיוון ההסתכלות הרצוי חווים נחות גדול יותר בתדרים הגבוהים ביחס לתדרים הנמוכים, דבר שגורם לעיוות לא רצוי של אות המוצא ולפגיעה באיכות האות הכוללת. כדי להתמודד עם בעיה זו, הוצעו בספרות מספר שיטות לעיצוב מעצבי אלומה עם רוחב אלומה קבוע או בלתי תלוי בתדר. עם זאת, חלק מהשיטות הללו כרוכות במורכבות חישובית גבוהה, מה שהופך אותן לבלתי ישימות ביישומים בזמן אמת, במיוחד כאשר מדובר במערכים גדולים או במגבלות חומרה מחמירות. שיטות אחרות מניחות כי כיוון ההגעה של האות הרצוי נמצא במישור האופקי בלבד, דבר שמגביל את יעילותן בסביבות תלת-ממדיות ופוגע משמעותית במדדים חשובים כמו מקדם כיווניות והגבר רעש לבן. בנוסף, לגאומטריית המערך יש השפעה מכרעת על ביצועי המערכת הכוללים.

עבודת תיזה זו מתמקדת בתכן יעיל של מעצבי אלומה בעלי רוחב אלומה קבוע באווית העילוי, המיושמים על מערכי טבעות קונצנטרים. אנו מאמצים את תצורת מערך הטבעות הקונצנטרים, שבה מבוצעת סכימה אנלוגית של כל האותות הנקלטים על ידי כל מיקרופון בטבעת, עוד לפני הדגימה. אף על פי שתכן זה מבטל את יכולת ניהוג האלומה, הוא דורש פחות משאבים ומפשט באופן משמעותי את המורכבות החישובית הכוללת, מה שהופך אותו למתאים במיוחד ליישומים בזמן אמת ובסביבות עם מגבלות משאבים. בנוסף לכך, מסנני מעצב האלומה ממומשים באמצעות מסנני תגובת הלם סופית בתחום הזמן, דבר המתאים יותר ליישומים בזמן אמת הדורשים השהיות קטנות במיוחד. ראשית, אנו מציגים בעיית תכנות ריבועית קמורה עבור תצורת מערך טבעות קונצנטרים נתון. מוצעים מספר אילוצים לצורך עיצוב מדויק של תגובת המערך, שמירה על רוחב אלומה קבוע על פני טווח רחב של תדרים, ותגובה נטולת עיוותים בכיוון ההגעה של האות הרצוי. נעשה שימוש בייצוג פאזה רציפה של מסנני תגובת הלם סופית המאפשר אופטימיזציה ישירה ומשותפת של מקדמי המסנן בתחום הזמן לכל הטבעות. פונקציית המטרה המוצעת מכילה משתנה שליטה, המאפשר איזון



המחקר בוצע בהנחייתו של פרופסור ישראל כהן בפקולטה להנדסת חשמל ומחשבים.  
חלק מן התוצאות בחיבור זה פורסמו כמאמר מאת המחבר ושותפו למחקר בכתב-עת במהלך תקופת  
מחקר המגיסטר של המחבר, אשר גרסתו העדכנית ביותר הינה:

O. Peretz and I. Cohen, "Constant elevation-beamwidth beamforming with concentric ring arrays," *IEEE/ACM Transactions on Audio, Speech, and Language Processing*, vol. 32, pp. 1662–1672, 2024.

מחבר חיבור זה מצהיר כי המחקר, כולל איסוף הנתונים, עיבודם והצגתם, התייחסות והשוואה  
למחקרים קודמים וכו', נעשה כולו בצורה ישרה, כמצופה ממחקר מדעי המבוצע לפי אמות המידה  
האתיות של העולם האקדמי. כמו כן, הדיווח על המחקר ותוצאותיו בחיבור זה נעשה בצורה ישרה  
ומלאה, לפי אותן אמות מידה.

## תודות

עבודה זו נעשתה תחת הנחייתו של פרופסור ישראל כהן בפקולטה להנדסת חשמל ומחשבים.  
ברצוני להביע את תודתי והערכתי העמוקה למנחה המחקר שלי, פרופ' ישראל כהן, על ההזדמנות,  
ההנחיה, התמיכה והסבלנות שלו לאורך שלבי המחקר. המומחיות, ההדרכה והתמיכה שלו הפכו אותי  
לחוקר טוב יותר באופן משמעותי.  
לבסוף, אני רוצה להודות למשפחתי על התמיכה והעידוד בתהליך הזה. הישג זה לא היה אפשרי  
בלעדיהם.

אני מודה לטכניון, לתוכנית המחקר המשותפת של הקרן הלאומית למדע והקרן הלאומית למדעי  
הטבע של סין (מענק מס' 1449/23), ולקרן פזי על התמיכה הכספית הנדיבה בהשתלמותי.



# תכנן של מעצבי אלומה לרוחב אונה ראשית קבועה בזווית הגבהה עם מערכי טבעות קונצנטריים

חיבור על מחקר

לשם מילוי חלקי של הדרישות לקבלת התואר  
מגיסטר למדעים בהנדסת חשמל

אוראל פרץ

הוגש לסנט הטכניון – מכון טכנולוגי לישראל  
אייר התשפ"ה חיפה מאי 2025



**תכן של מעצבי אלומה לרוחב אונה ראשית  
קבועה בזווית הגבהה עם מערכי טבעות  
קונצנטריים**

**אוראל פרץ**